ARTICLE

All-atom Molecular Dynamic Simulations and NMR Spectra Study on Intermolecular Interactions of N,N-dimethylacetamide-Water System

Rong Zhang*, Zai-you Tan, San-lai Luo

Lab of Physical Chemistry, College of Pharmacy, Guangdong Pharmaceutical University, Guangzhou 510006, China

(Dated: Received on October 21, 2007; Accepted on January 2, 2008)

N,N-dimethylacetamide (DMA) has been investigated extensively in studying models of peptide bonds. An all-atom MD simulation and the NMR spectra were performed to investigate the interactions in the DMA-water system. The radial distribution functions (RDFs) and the hydrogen-bonding network were used in MD simulations. There are strong hydrogen bonds and weak C−H···O contacts in the mixtures, as shown by the analysis of the RDFs. The insight structures in the DMA-water mixtures can be classified into different regions by the analysis of the hydrogen-bonding network. Chemical shifts of the hydrogen atom of water molecule with concentration and temperatures are adopted to study the interactions in the mixtures. The results of NMR spectra show good agreement with the statistical results of hydrogen bonds in MD simulations.

Key words: All-atom simulation, NMR spectrum, DMA-water system, Hydrogen bond

I. INTRODUCTION

Interactions among the peptide groups play essential role in the structures and properties of biological systems, such as proteins and nucleic acids [1-3]. Simple amide systems have been investigated extensively as the models of peptide bonds because of their presence as a repeating unit in biological macromolecules and some polymers [4-8]. Recently, it has been recognized that C−H···O interactions play a significant role in determining the molecular conformation and stabilization of complexes, and in the activity of biological macromolecules [9,10].

Molecular dynamics (MD) simulation has proven to be particularly valuable for studying structures and interactions in mixtures [11-13]. Spectral measurements such as NMR spectra are highly powerful techniques which can be used to investigate structures and interactions in the mixtures [14-17]. On the other hand, a variety of experimental and theoretical methods have been carried out to study the hydrogen bonding of N,N-dimethylacetamide (DMA) since it is a simple molecule containing the C=O···H−N characteristic of the peptide bond [18-22]. Takamuku and co-workers [18] adopted IR, X-ray diffraction, and mass spectrometry to investigate aqueous mixtures of DMA, and one interesting behavior of the mixtures was found: that anomalies occur at $x_{\mathrm{DMA}}\approx 0.33$ in the mixtures. Also, Verbovy and co-workers [20] used FTIR to study ion solvation in electrolyte solutions in DMA molecules.

In previous works, we have investigated the interactions and structures in the amide-water system such as N-methylacetamide (NMA) and N,N-dimethylformamide (DMF) [6,23,24]. Some interesting phenomena were observed in the mixture, for instance, the two methyl groups in amide molecule are found to show different capabilities in forming weak C−H···O contacts in the mixtures from the radial distribution functions (RDFs). Furthermore, the temperature-dependent NMR results of the different methyl groups also show excellent agreement with the MD simulations.

In the present work, we adopted an all-atom MD simulation and NMR spectra to investigate the intermolecular interactions in the DMA-water system. The RDFs and the statistics of hydrogen bonding networks and chemical shifts were used to reveal the interactions and structures in the DMA aqueous solutions. Mixtures of liquids can be simulated by using the interaction potentials of the pure liquids. The results should be viewed as providing a qualitative description of DMA-water mixtures. Moreover, it remains an important task to compare the experimental and predicted properties of the mixtures.

II. COMPUTATIONAL METHODS

A. Molecular models

Simple potential models were used for DMA and water. The nonbonded interactions are represented by a sum of the Coulomb and Lennard-Jones terms with Eq.(1)

$$E_{\mathrm{ab}}=\sum_{i}^{\mathrm{a}}\sum_{j}^{\mathrm{b}}\left[\frac{q_i q_j e^2}{r_{ij}}+4\varepsilon_{ij}\left(\frac{\sigma_{ij}{}^{12}}{r_{ij}{}^{12}}-\frac{\sigma_{ij}{}^{6}}{r_{ij}{}^{6}}\right)\right]f_{ij} \qquad (1)$$

*Author to whom correspondence should be addressed. E-mail: zhangr@china.com.cn

where E_{ab} is the interaction energy between molecules a and b. Standard combining rules are used via Eq.(2).

$$\sigma_{ij} = (\sigma_{ii}\sigma_{jj})^{1/2}, \quad \varepsilon_{ij} = (\varepsilon_{ii}\varepsilon_{jj})^{1/2} \tag{2}$$

The same expression is used for intramolecular nonbonded interactions between all pairs of atoms ($i<j$) separated by three or more bonds. In Eq.(1), f_{ij}=1.0 except for intramolecular 1,4 interactions for which f_{ij}=0.5.

SPC model [25] for water molecule and OPLS-AA [26,27] (optimized potentials for liquid simulations-all atom) model are used for DMA molecules. N-methyl group parameters are somewhat changed to agree well with experimental values of the density and heat of vaporization so that OPLS-AA work will be hardly affected. The calculated potential parameters for the pure components were set using the data in the previous work [24]. The potential parameters and symbol of the atom in the molecules are given in Table I. The structure of DMA molecule is shown in Fig.1.

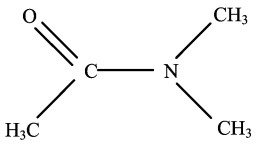

FIG. 1 Structure of DMA molecule.

TABLE I Potential parameters [23] and symbol of the atoms for SPC water and DMA

Solvent	Atom	σ/Å	E/(kJ/mol)	q/e
Water	OW	3.1656	0.1554	−0.8200
	HW	0.0000	0.0000	0.4100
DMA	C (C=O)	3.7500	0.1050	0.5000
	O	2.9600	0.2100	−0.5000
	N	3.2500	0.1700	−0.1400
	C1 (C−CH_3)	3.5000	0.0660	−0.1800
	C2 (N−CH_3)	3.5000	0.0660	−0.1100
	H1 (C−CH_3)	2.4200	0.0150	0.0600
	H2 (N−CH_3)	2.5000	0.0300	0.0600

B. Simulation Details

MD calculations were performed by a modified TINKER 4.2 molecular modeling package [28]. The simulations were carried out in the NPT ensemble at T=298 K and p=101.3 Pa with a total of 512 molecules with the mole fraction of DMA molecules at 0.1, 0.2, 0.35, 0.5, 0.65, 0.8, and 0.95. Periodical boundary conditions were used together with a sphere cutoff. The SHAKE algorithm was applied to constrain the bond length of the DMA molecules, and the SETTLE algorithm was used to constrain the water geometry. The energies of the initial configurations were minimized using the MINIMIZE program in the TINKER 4.2 package. The time step was 1 fs and the configurations were saved every 0.1 ps for analysis. The mixtures were sufficiently equilibrated to ensure that there were no systematic drifts in the potential energies with time. The equilibrations were followed by monitoring the RDFs as well as the fraction of molecules of each species that had a given number of hydrogen bonds. The statistics were collected during the last 100 ps.

C. Definitions

An analysis of hydrogen bonding networks was used to gain deeper insight into the aqueous structures. Here we used geometric criteria that are the same as those used by Luzar and Chandler [29], such as a typical criterion of neat water: r(OW$\cdots$HW)≤2.45 Å, r(OW$\cdots$OW)≤3.60 Å, and the angle φ(HW−OW$\cdots$OW)≤30°. Although there have been a great number of researches, defining the weak C−H$\cdots$O hydrogen bond is still somewhat arbitrary. Different investigators have attempted to give some slightly different criteria for identifying such weak contact. For the weak contact C−H$\cdots$O, here is a geometrical criteria for C−H$\cdots$O contact of small molecules: r(O$\cdots$H)<2.8 Å, 3.0Å<r(O$\cdots$O)<4.0 Å and the angle φ(C−H$\cdots$O)>110° [30].

D. Experimental section

NMR spectrum analysis is a highly powerful technique which can be used to investigate structures and interactions in mixtures. NMR spectra were measured using a Bruker DMX 500 spectrometer operating at 500 MHz at different temperatures with an accuracy of ±0.1 °C. A 2-mm capillary tube, in which deuterated dimethyl sulfoxide (DMSO-d_6) was sealed, was placed at the center of a 5 mm sample tube filled with the chemical shift reference of sodium 2,2-dimethyl-2-silapentane-5-sulfonate (DSS) and the sample solution. The chemical shifts for ^{1}H atom of the DMA-water mixtures at temperatures of 298, 313, 328, and 343 K were measured.

III. RESULTS AND DISCUSSION

A. Thermodynamic properties of pure DMA and water

The density and heat of vaporization of the liquid are important in measuring the size of the molecules and the strength of the interaction. Density is easy to calculate in a periodic boundary system and simultaneously provides a good test of the intermolecular forces, the cutoff criterion, and the NPT method used. The density is calculated through the average volume with

DOI:10.1088/1674-0068/21/03/221-226

Eq.(3) [30]

$$\rho = \frac{M}{0.622}\frac{\langle V\rangle}{N} \tag{3}$$

where ρ is the density in g/cm^3, M is the molecular weight, N is the number of molecules in the periodic box, V is the calculated volume in Å^3, and 0.6022 is the unit conversion factor. The heat of vaporization can check directly the intermolecular energy of system, which is responsible for its state of aggregation. The heat of vaporization is well approximated from the calculated energy via Eq.(4) [30], where R is the gas constant and T is the absolute temperature.

$$\Delta H_{\rm vap} = -\frac{\langle E(l)\rangle}{N} + RT \tag{4}$$

In Table II, a summary of the calculated properties along with the experimental values is shown. The OPLS-AA model of pure DMA represents the experimental liquid density and the heat of vaporization very well. The agreement between the calculated and experimental values is also very good for the SPC model.

TABLE II Calculated and experimental thermodynamic properties of pure liquids

Liquid	$\Delta H_{\rm vap}$/(kJ/mol)		ρ/(g/cm^3)	
	Cal.	Exp.	Cal.	Exp. [19]
DMA	49.95	49.12 [26]	0.932	0.936
Water	43.18	43.93 [25]	0.983	0.994

B. $g(r)$ in DMA-water system

The all-atom simulations further give an insight into the local structure of DMA aqueous solution. The structure of the liquid can be characterized well by the RDF, $g(r)[x\cdots y]$, which gives the probability of finding an atom of type y at a distance r from an atom of type x. The $g(r)$ values of the whole concentration in DMA aqueous solutions are given in Fig.2. Some distinct peaks near 1.9 Å are observed in $g(r)$ [O$\cdots$HW]. The short distances and strong intensities show that the hydrogen bonds of C=O$\cdots$HW are very strong. The peaks of the second hydration shell are observed near 3.2 Å which imply that the DMA aqueous solutions are structured. Also, the first peaks near 2.8 Å of $g(r)$[OW$\cdots$H2] are obvious which shows that C$-$H$\cdots$O contacts exist in the DMA-water system. The broad peaks of the RDFs also imply that the intermolecular interactions are likely to include the weak hydrogen bonds as well as other weak interactions such as dipolar interactions and dispersions. So the weak C$-$H$\cdots$O contacts can not be neglected in amide-water mixtures even though the intensities of the weak C$-$H$\cdots$O contacts are weaker than those of the strong hydrogen bonds.

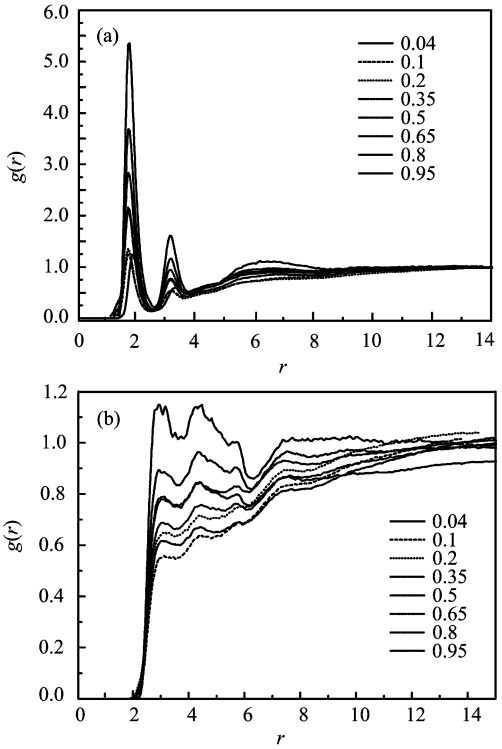

FIG. 2 RDF of DMA over the entire concentration range (mole fraction) in the DMA-water mixtures. (a) $g(r)$[O$\cdots$HW]. (b) $g(r)$[OW$\cdots$H2].

C. Hydrogen-bonding Network

As shown above, RDFs do not provide explicit information on ordering in binary mixtures, so we carried out a detailed analysis of hydrogen bonding networks in the mixtures to gain deeper insight into the aqueous structures. One basic aspect of the hydrogen bonding network is the probability distribution, describing the number and type of hydrogen bonds that a molecule is engaged in with other molecules. The hydrogen bonds of C=O$\cdots$HW and OW$\cdots$HW play crucial roles in aqueous solutions. Another important factor is the weak contacts of C$-$H$\cdots$O that also exist in the DMA aqueous solution. On the other hand, water molecules can be both donors and acceptors of hydrogen bonds, leading ideally to tetrahedral water coordination. The carbonyl and the water oxygen atoms compete as acceptors of hydrogen bonds. Moreover, the water and the hydrogen atoms in DMA compete as donors of hydrogen bonds. It is the competition of these hydrogen bonding interactions which leads to hydrogen bonding networks in the DMA-water mixtures. The hydrogen bonds are determined by a similar geometrical criterion to that of pure water as defined above. A summary of the statistics is given in Fig.3. For the strong hydrogen bond of C=O$\cdots$HW which is given in Fig.3(a), it is found that the free carbonyl oxygen atoms increase with $x_{\rm DMA}$, and the fractions of cluster for the carbonyl oxygen atom ac-

DOI:10.1088/1674-0068/21/03/221-226

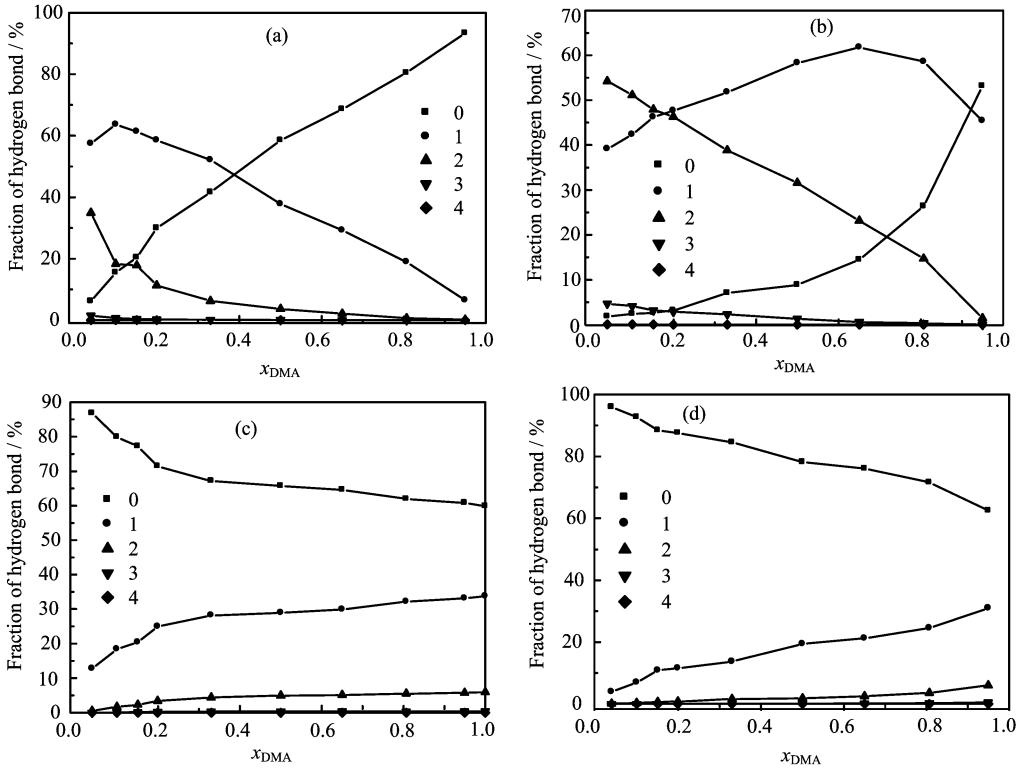

FIG. 3 Hydrogen-bonding network in DMA-water system. (a) C=O···HW. (b) OW···HW. (c) O···H2. (d) OW···H2.

cepting one or two protons of water are high in the water rich region. These indicate that the carbonyl oxygen easily forms hydrogen bonds with hydrogen atoms of water molecules, as well as being a good proton acceptor. For another hydrogen bond of OW···HW shown in Fig.3(b), the free oxygen of water also increases with x_{DMA}. The aggregate of OW accepting two protons of water is in a high level in the water rich region, and then decreases with the x_{DMA}. In Fig.3(c) and (d), the aggregates of O and OW atom accepting one methyl proton both increase with x_{DMA} which implies that the weak C−H···O contacts are not dominated in the water rich region. Because there is no active hydrogen atom in DMA, the oxygen atom of water prefers its own hydrogen atoms as acceptors. Also, the atom of HW can form the hydrogen bonds with atoms of OW or O. In the water rich region, the water molecules prefer to form hydrogen bonds with themselves. Therefore, the stable water clusters predominate. With the DMA increasing, the structure of the water cluster is broken down, and there exist clusters with across association. Then in the DMA rich region, DMA clusters become dominant.

D. NMR experiment

Spectral measurements such as IR, Raman, and NMR are highly powerful techniques that may be used to investigate intermolecular interactions in solution. However, there is still little spectral data over the whole composition range for binary mixtures, especially in aqueous mixtures. NMR spectra are often used to investigate intermolecular interactions in solution. It is well known that the effect on the chemical shift of hydrogen bonds is much larger than all of the other intermolecular interaction effects. Since the chemical shift is a measure of the electron density about the probe nuclei, it gives the information state for the atom. Chemical shift will move to low field and the value will become larger when forming hydrogen bonds [15,16]. Thus, the variety of the chemical shifts can reflect the capability of forming hydrogen bonds. In the present work, we got the chemical shifts of the whole concentration for the DMA aqueous solution at the temperature of 298, 313, 328, and 343 K.

The comparison between the average number hydrogen bonds in MD simulation and chemical shifts of hydrogen atom of water molecule with the concentration are given in Fig.4. The chemical shift of water protons, δ_{HW}, is a measure of the electron density for the water protons, and it reflects the polarization of water molecules dissolving solutes. The water molecules are apt to be more structured in the water rich region and the local tetrahedral coordination of water leads to a "breakdown" with x_{DMA}. The atom of HW can form strong hydrogen bonds of O···HW and OW···HW with the concentration which will lead to the variety in chemical shifts. In Fig.4, it is found that

DOI:10.1088/1674-0068/21/03/221-226

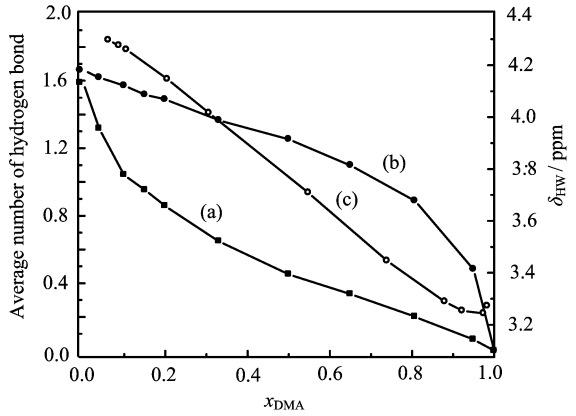

FIG. 4 Comparison between the average number of hydrogen bonds for (a) O···HW and (b) OW···HW. (c) The chemical shifts for atom of HW at 298 K.

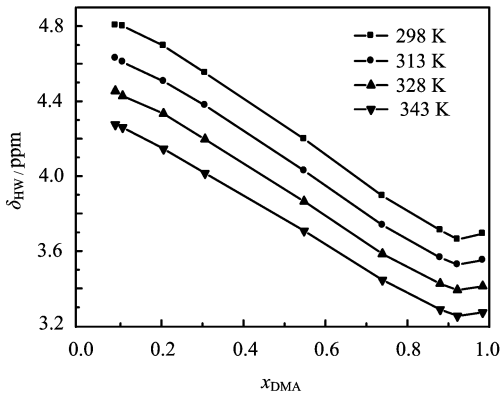

FIG. 5 δ_{HW} in DMA-water system at different temperatures.

the average numbers of hydrogen bonds for O···HW and OW···HW are both decrease with x_{DMA}. On the other side, the values of δ_{HW} are also becoming smaller with x_{DMA}. So the two results of the NMR experiment and the MD simulations represent consistent concentration dependencies.

Hydrogen bonding interactions are also sensitive to temperature [15,16,23]. The variety of the chemical shifts in NMR can also reflect the change of the hydrogen bonds in DMA aqueous solution. Chemical shift moves to high field and the value becomes smaller with the temperature increasing. Strong hydrogen bonds lead to greater shift than weak hydrogen bonds. The varieties of the chemical shifts with temperature also reflect the capabilities of forming hydrogen bonds. The values of δ_{HW} with temperatures are shown in Fig.5. Due to formation of strong hydrogen bonds, the varieties of δ_{HW} become larger with temperature. Moreover, the varieties in the water rich region are greater than those in the DMA rich region, which reflects the fact that more hydrogen bonds of OW···HW are formed in the water rich region. That is to say, the stable water clusters dominate in the water rich region which is also in agreement with the results of the analysis in the hydrogen-bonding network. The result of the NMR experiment shows good agreement with the MD simulations.

IV. CONCLUSION

An all-atom MD simulation combined the NMR experiment was performed to investigate the structures and interactions in the DMA-water system. The results of RDF indicate that strong hydrogen bonds and the weak C−H···O contacts both exist in the DMA-water mixture. The water oxygen and the carbonyl atoms compete as acceptors of hydrogen bonds, and the hydrogen atoms in DMA or water compete as donors of hydrogen bonds. It is the competition of these hydrogen bonding interactions which leads to hydrogen bonding networks in the DMA-water mixtures. Through the analysis for hydrogen-bonding network, the mixtures can be classified into different regions: in the water rich region, the stable water clusters dominate; with the DMA increasing, the structure of the water cluster is broken down, and there are aggregates of the across associate between the water and DMA in the mixture; in the DMA rich region, the DMA clusters become dominant. Moreover, the statistical average number of hydrogen bonds and chemical shifts in NMR represent the consistent concentration dependencies. The temperature-dependent NMR results also show good agreement with analysis of the hydrogen-bonding network. All-atom MD simulations and NMR spectra are successful in revealing the structures and interactions in the DMA-water mixtures.

V. ACKNOWLEDGMENTS

This work was supported by the Doctoral Scientific Research Foundation of the Natural Science Foundation of Guangdong Province, China (No.7301567) and the Research Foundation of Guangdong Pharmaceutical University, China (No.2006YKX05).

[1] A. N. Drozdov, A. Grossfield, and R. V. Pappu, J. Am. Chem. Soc. **126**, 2574 (2004).
[2] B. R. Huck, J. D. Fisk, I. A. Guzei, H. A. Carlson, and S. H. Gellman, J. Am. Chem. Soc. **125**, 9035 (2003).
[3] L. A. Ralat, Y. Manevich, A. B. Fisher, and R. F. Colman, Biochemistry **45**, 360 (2006).
[4] R. Vargas, J. Garza, R. A. Friesner, H. Stern, B. P. Hay, and D. A. Dixon, J. Phys. Chem. A **105**, 4963 (2001).
[5] M. Buck and M. Karplus, J. Phys. Chem. B **105**, 11000 (2001).

DOI:10.1088/1674-0068/21/03/221-226

[6] R. Zhang, H. Li, Y. Lei, and S. Han, J. Mol. Struc. **693**, 17 (2004).
[7] M. Chalaris and J. Samios, J. Chem. Phys. **112**, 8581 (2000).
[8] T. Köddermann and R. Ludwig, Phys. Chem. Chem. Phys. **6**, 1867 (2004).
[9] Y. Gu, T. Dar and S. Scheiner, J. Am. Chem. Soc. **121**, 9411 (1999).
[10] R. Vargas, J. Garza, D. A. Dixon, and B. P. Hay, J. Am. Chem. Soc. **122**, 4750 (2000).
[11] K. Lee, D. R. Benson, and K. Kuczera, Biochemistry **39**, 13737 (2000).
[12] J. Gao, J. J. Pavelites, and D. Habibollazadeh, J. Phys. Chem. A **100**, 2689 (1996).
[13] A. Vishnyakov, A. P. Lyubartsev, and A. Laaksonen, J. Phys. Chem. A **105**, 1702 (2001).
[14] S. H. Gellman, G. P. Dado, G. B. Liang, and B. R. Adams, J. Am. Chem. Soc. **113**, 1164 (1991).
[15] K. Mizuno, S. Imafuji, T. Fujiwara, T. Ohta, and Y. Tamiya, J. Phys. Chem. B **107**, 3972 (2003).
[16] K. Mizuno, Y. Kimura, H. Morichika, Y. Nishimura, Y. Shimada, S. Maeda, S. Imafuji, and T. Ochi, J. Mol. Liq. **85**, 139 (2000).
[17] K. Mizuno, S. Imafuji, T. Ochi, T. Ohta, and S. Maeda, J. Phys. Chem. B **104**, 11001 (2000).
[18] T. Takamuku, D. Matsuo, M. Tabata, T. Yamaguchi, and N. Nishi, J. Phys. Chem. B **107**, 6070 (2003).
[19] W. Xu, F. Mao, H. Zhao, Y. Wang, and J. Wang, J. Chem. Eng. Data **52**, 553 (2007).
[20] D. M. Verbovy, T. G. Smagala, M. A. Brynda, and W. R. Fawcett, J. Mol. Liq. **129**, 13 (2006).
[21] P. Sivagurunathan, K. Ramachandran, and K. Dharmalingam, Acta Phys. Chim. Sin. **23**, 295 (2007).
[22] M. Johnson, M. Kalidoss, and R. Srinivasamoorthy, J. Chem. Eng. Data **47**, 1388 (2002).
[23] R. Zhang, H. Li, Y. Lei, and S. Han, J. Phys. Chem. B **108**, 12596 (2004).
[24] R. Zhang, H. Li, Y. Lei, and S. Han, J. Phys. Chem. B **109**, 7482 (2005).
[25] H. J. C. Berendsen, J. P. M. Postma, W. F. van J. Gunsteren, and M. Hermans, *In Intermolecular Forces* Reid: Dordrecht, 331 (1981).
[26] W. L. Jorgensen, D. S. Maxwell, and J. Tirado-Rives, J. Am. Chem. Soc. **118**, 11225 (1996).
[27] W. L. Jorgensen and C. Swenson, J. Am. Chem. Soc. **107**, 1489 (1985).
[28] M. J. Dudek, K. Ramnarayan, and J. W. Ponder, J. Comput. Chem. **19**, 548 (1998).
[29] A. Luzar and D. Chandler, J. Chem. Phys. **98**, 8160 (1993).
[30] Y. Lei, H. Li, H. Pan, and S. Han, J. Phys. Chem. A **107**, 1574 (2003).

DOI:10.1088/1674-0068/21/03/221-226